Tellus (2006), 58B, 117–128
Printed in Singapore. All rights reserved

TELLUS

Effect of climatic changes and human activity on soil carbon in desertified regions of China

By QI FENG*, WEI LIU, ZHANG YANWU, SI JIANHUA, SU YONGHONG, CHANG ZUN QIANG and XI HAIYANG, *Cold and Arid Regions Environmental and Engineering Research Institute, Chinese Academy of Sciences, No. 260 West Duong Gang Road, Lanzhou 730000, P. R. China*

(Manuscript received 17 January 2005; in final form 23 August 2005)

ABSTRACT

A total of 340 soil samples from 17 different types of sandy land regions in China were analyzed for soil organic carbon (SOC). Stepwise regression served to identify correlations between SOC and a number of climatic factors measured at the sampling sites: winter, summer, nighttime and daytime air temperatures (AT) and precipitation. In desertified lands SOC showed a direct correlation with precipitation, but no significant relationship with the mean air temperature. However, in northwest and northeast China decreases in SOC were linked to rises in day/night and seasonal temperatures, while in north China they were linked to a rise in mean temperature. Over the entire study period (1950–1990), precipitation in the region decreased by 25 mm decade^{-1}, while the mean air temperature increased by 0.14°, 0.28° and 0.15° decade^{-1} in the northwest, northeast and north central regions, respectively. Driven by rises in day/night and seasonal temperatures, long-term alterations to global ecosystem processes, particularly the carbon cycle, may significantly alter the number and diversity of plants in desertified ecosystems. Based on multiple regression analysis, over the past 40 years, about 20% of emissions from SOC in the northeast were attributable to air temperature; in the north central region 31 and 16% of emissions were attributable to precipitation and mean AT, respectively; while in the northwest 28, 18 and 32% of the emissions were attributable to mean AT, nighttime temperature, and decreasing precipitation, respectively. It is obvious that human activities are the main single causative factor in the release of SOC-derived greenhouse gases to the atmosphere from desertified areas.

1. Introduction

Improved estimates of soil organic carbon (SOC) are needed to calculate current regional, continental and global soil carbon stores (Schlesinger, 1984; Burke et al., 1989; Kern, 1994). Global climate changes due to increasing concentrations of greenhouse gases are further emission by the deforestation of the world's tropical regions (Vogt et al., 1995), which, along with arctic regions, have been the focus of much attention. However, changes in soil carbon stores are also to be expected in other climatic regions. Many efforts have been made to determine changes in SOC storage induced by changes in land use at the regional level (Bon, 1976; Wu et al., 2003). Given the lack of baseline soils data, the inherent natural variability of soils and their carbon exchange dynamics under different land uses, few detailed studies of SOC have been published (Lal, 1999; Wu et al., 2003). Indeed, there is a great need for more accurate and wide-ranging studies of current SOC storage and the effects of human activity thereon (Bruce et al., 1999; Wu et al., 2003).

*Corresponding author.
e-mail: qifeng@ns.lzb.ac.cn

Emanuel et al. (1985) estimated that there would be a 17% increase in world desert land area because of the climate changes expected with a doubling of the atmospheric CO_2 content. A shift towards a greater area of arid land potentially represents a permanent loss in the productive capacity of the biosphere (Schlesinger et al., 1990). However, no detailed analysis has yet addressed the relationship between SOC and environmental factors in desertified lands, and in particular not in those of northern China. Environmental and meteorological conditions resulting from desertification in this region could have serious effects in Asia, and even in the Pacific Ocean and North America, where greater airborne dust flow and deposition could occur.

As desertified land soils are sensitive to changes in the environment and in vegetative cover, it is particularly important to identify the variability of SOC in soil profiles up to 1.0 m in depth. To date, losses of agricultural productivity and the associated social and economic disruptions during droughts cannot be said to represent desertification, unless the landscape is so altered that a full recovery during relatively moist conditions is impossible (Schlesinger et al., 1990). The widely distributed desertification-prone lands of northern China present remarkable æolian landforms, and it is such sand desertification or sand encroachment

that we consider as symptomatic of desertification. Some studies have highlighted the important role of China's terrestrial ecosystems in the global carbon cycle (Peng and Apps, 1997; Fang et al., 2001; Wu et al., 2003), with some having specifically estimated changes of SOC in tropical–subtropical (Li and Wang, 1998; Li and Zhao, 2001) and northern regions (Wang et al., 1998a; Feng et al., 2001a) of China. While Wu et al., (2003) presented a comprehensive nationwide estimate of anthropogenic changes in SOC storage, no study has as yet reported on the relationship existing between SOC and environmental factors in the desertified lands of northern China. In our study, we determined the variability of SOC within different climatic zones of northern China, across soil depths of 0–0.2 m or 0–1.0 m. For lands in northern China undergoing or having undergone desertification, a detailed analysis of the relationship between SOC and environmental factors, particularly those linked to global warming (precipitation, temporal changes in air temperature and human activity) was also undertaken.

The paper is organized as follows. In Section 2 methods and materials are discussed. The results are presented in Section 3, followed by a discussion in Section 4. Conclusions are found in Section 5.

2. Methods and materials

Vast regions of desertification-prone lands exist in China, covering a total land area of 334 000 km^2. They are mainly situated in northern China, between 75°–125°E and 35°–50°N (Fig. 1; Feng et al., 2001a). The desertification-prone lands, whose surface features are denuded by wind and where farmlands are covered by thin sheets of sand and eroded material, occur in a number of different climatic zones: subhumid, semiarid and arid desert (Zhu et al., 1988). On the basis of field investigations, desertification-prone lands were described as forerunner, decayed, degenerated and devastated (Table 1). Forerunner lands retained their ecosystem structure as determined by climatic zones, and showed relatively stable energy and substrate cycling. Decayed lands showed reductions in biological diversity of the ecosystem, transformation rate of organic substrates in the soil, and biological productivity (biomass) to 70–80% of forerunner lands. Degenerated lands presented incomplete ecosystems, inhibited substrate transformations, lowered ability to regenerate and a biomass production only 30–40% of that of forerunner lands. Devastated lands exhibited inoperative metabolic linkages within the ecosystem, loss of basic metabolic functions and biomass production less than 10% of that of forerunner lands. Severely desertified land refers to regions where surface features are denuded by wind erosion and farmlands covered by thin sheets of sand.

Variations in SOC were identified in different desertification-prone lands of northern China by obtaining a total of 340 soil samples distributed in 136 soil profiles (0–1.0 m or 0–0.2 m). These were used to ascertain whether emissions from SOC were most closely related to site type or to temperature and precipitation variations in the region. Forty-year mean precipitation (P), air temperature (AT) and soil bulk density (ρ) data were used

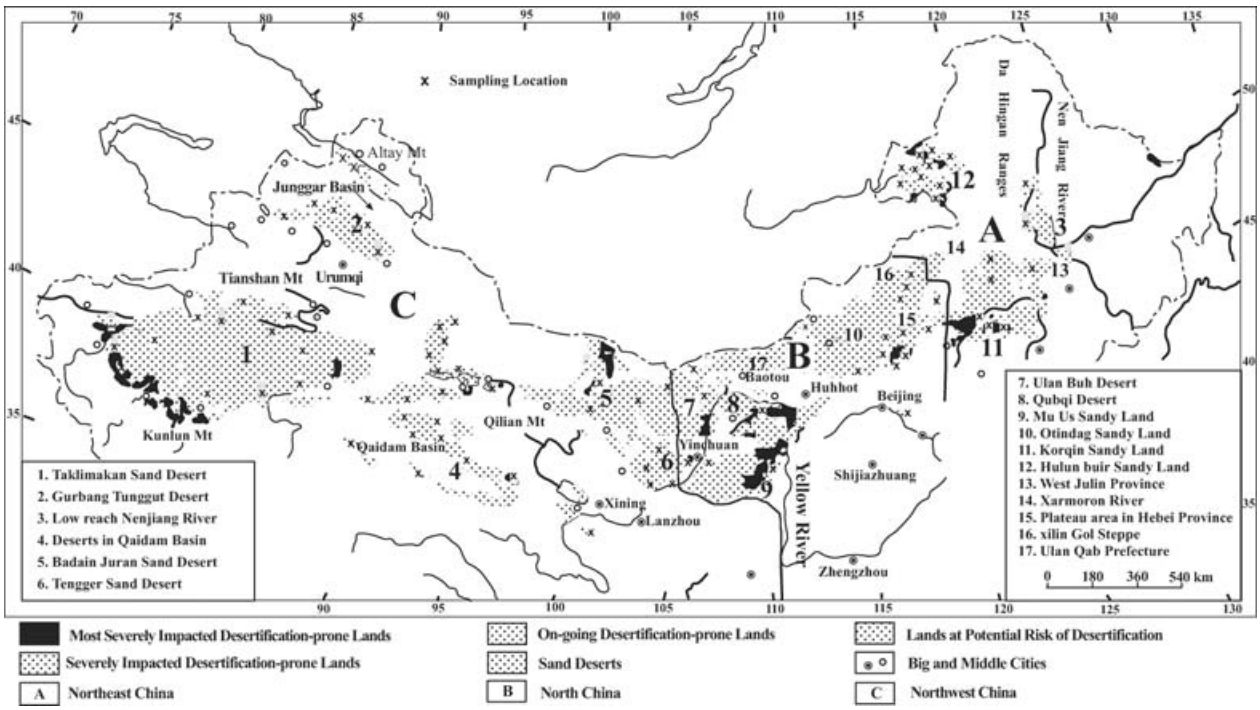

Fig 1. The sketch map of northwest, northeast and north China and the distribution of sandy lands.

Table 1. Status of ecosystem in the cases of different intensities of desertification

Proneness to desertification	Latent	On-going	Severe	Most severe
Damage level to the ecosystem	Forerunner (FOR)	Decayed (DEC)	Degenerated (DEG)	Devastated (DEV)
Status of ecosystem: structure and function	Ecosystem structure suited to zonal site	The decrease in biological loads and diversity	The basic composition of ecosystem incomplete	Network of substrate metabolism links gone
	The system possesses relative stable energy and material cycling	Poor substrate transformation rate and decreasing biomass	Substrate transformation impeded, decreased ability for regeneration	Basic metabolic functions lost

in an attempt to develop significant linear relationships (SAS Institute, 1985) linking these parameters and SOC.

The mean organic matter content for each 0.1-m soil layer was calculated from three replicate samples, and the means summed to obtain the total organic matter content of the entire 1.0 m of the topsoil layer. These measurements to calculate the total (released and stored) amounts of carbon as

$$C_{\text{tot}} = Ah\rho C_{\text{org\%}}, \tag{1}$$

where

C_{tot} is the total carbon content stored in the top 1.0-m layer of the desertified land (kg),
A is the area of the desertified land (km^2),
h is the mean depth (cm),
ρ is the bulk density (mg m^{-3}) and
$C_{\text{org\%}}$ is the mean organic carbon content (%).

In those cases when only the organic matter content was measured, it was multiplied by the dimensionless Bemmelen Index (Wolff, 1864; van Bemmelen, 1890) of 0.58 to determine the mean organic carbon, o. The mean and standard deviation of organic carbon contents in the top 1.0-m soil layer of sandy lands in China are shown in Table 2, while those of different land areas are presented in reference (Feng et al., 2002).

To estimate the area of the soil types and of the major deserts, sandy lands, and vegetation types of northern China, photocopies of large-scale maps were cut out according to these regions. The pieces of paper were then weighed to the nearest 0.1 mg, and the mass representing known land areas were converted to km^2. Soil data were complied from several decades of soil mapping and survey throughout northern China. According to these methods, the total area of north China calculated as the sum of soil groups, of land area and of vegetation groups agreed with the actual areas within 1% in both cases. The mean annual growth or developmental rate of desertification-prone lands was expressed as

$$R = n[Q_2/(Q_1 - 1)] \times 100, \tag{2}$$

where

R is the mean annual growth rate of desertification-pronelands,
Q_1 is the percentage of aolian landforms in the total land area calculated from the initial ae rial photos,
Q_2 is the percentage of aolian landforms in the total land area calculated from the final ae rial photos and
n is the time between the initial and final ae rial photos.

Based on the mean annual growth rate of desertification-prone lands, the areas of the different land types in a certain region during a certain year were calculated as

$$A_{\text{pred}} = A_{\text{init}}(1 + R)n', \tag{3}$$

where

A_{pred} is the predicted area of desertification-prone land at a given date (e.g. 2030) (km^2),
A_{init} is the known area of desertification-prone land at a given initial time (km^2)and
n' is the duration from the initial time to that at which the area is predicted (years) (Zhu et al., 1988).

In case of desertification being reversed through the application of artificial measures, the area of desertification-prone land in a region up to a certain time can be calculated as

$$A_{\text{pred}} = A_{\text{init}}(1 - R)n'. \tag{4}$$

Based on eqs. (1)–(4), the net carbon balance of desertification-prone lands between 1950 and 1990 is given in the reported (Feng et al., 2002).

Table 2. Calculation of the organic carbon content in the top 1 m soil layer of sandy lands in China

Sandy lands[a] region	Type (vegetation cover %)[b]	Area (km^2)	Bulk density ($mg\ m^{-3}$)	Mean depth ($m\ 10^{-2}$)	Organic matter (%)	Mean org-C ($kg\ m^{-2}$)	Total carbon (Tg C)(SD)
Hulun	FOR (96)	4266	1.38	99.8	1.136	9.09	388.0 (0.74)
Buir	DEC (72)	3481	1.38	100.0	0.598	4.80	167.0(1.1)
sandy land	DEG (33)	275	1.39	100.0	0.434	3.50	9.6((0.85)
	DEV (8)	43	1.37	100.0	0.150	1.20	0.5(0.68)
Lower	FOR (98)	1501	1.36	100.0	1.122	8.90	134.8(1.2)
reach	DEC (76)	3286	1.39	100.0	0.619	4.95	162.8(1.32)
Nenjiang	DEG (37)	218	1.81	100.0	0.505	5.30	11.6(0.89)
River	DEV (9)	–	–	–	–	–	–
West Jilin	FOR (98)	4512	1.38	100.0	1.108	8.90	400.1(0.65)
Province	DEC (78)	5500	1.39	99.3	0.583	4.67	256.6(0.88)
	DEG (35)	209	1.35	102.0	0.423	3.39	7.1(1.10)
	DEV (–)	–	–	–	–	–	–
Horqin	FOR (92)	5440	1.37	100.7	0.812	6.50	353.6(1.50)
sandy land	DEC (73)	17675	1.39	99.3	0.427	3.42	604.1(1.2)
	DEG (33)	3917	1.36	101.4	0.310	2.48	97.2(1.15)
	DEV (7)	1175	1.38	99.8	0.184	1.47	17.3(0.87)
Upper	FOR (90)	7793	1.36	100.8	0.605	4.80	377.4(0.53)
reaches of	DEC (73)	3975	1.38	100.0	0.312	2.50	99.3(0.78)
Xarmoron	DEG (32)	1875	1.35	100.5	0.237	1.90	35.6(0.86)
River	DEV (5)	1625	1.35	100.0	0.064	0.50	8.3(0.91)
Plateau	FOR (98)	5536	1.37	100.7	1.564	12.5	693.0(1.12)
area in	DEC (79)	6699	1.37	100.6	1.000	8.00	536.2(0.57)
Hebei	DEG (36)	430	1.38	100.0	0.552	4.42	19.0(0.68)
province	DEV (–)	–	–	–	–	–	–
Xilin Gol	FOR (90)	47687	1.36	100.9	0.201	1.60	767.2(0.74)
Steppe	DEC (70)	8587	1.30	100.0	0.106	0.80	72.9(0.88)
	DEG (30)	7200	1.73	102.9	0.063	0.50	36.3(1.56)
	DEV (6)	1075	1.30	102.0	0.026	0.20	2.2(1.32)
Ulan Qab	FOR (90)	4028	1.30	105.3	0.189	1.50	60.9(0.66)
Prefecture	DEC (72)	3837	1.35	102.7	0.097	0.78	29.8(0.35)
	DEG (31)	30	1.36	102.0	0.071	0.57	0.2(0.87)
	DEV (–)	–	–	–	–	–	–
Ulan Buh	FOR (90)	19200	1.32	101.2	0.129	1.00	198.2(1.45)
Desert	DEC (71)	256	1.33	103.0	0.068	0.54	1.4(1.22)
	DEG (32)	320	1.38	99.4	0.049	0.39	1.3(1.54)
	DEV (2)	208	1.35	97.7	0.017	0.13	0.3(0.99)
Mu Us sandy	FOR (91)	5840	1.38	100.2	0.106	0.85	49.5(0.52)
land	DEC (70)	8964	1.30	107.0	0.056	0.45	40.2(0.32)
	DEG (31)	4590	1.39	99.2	0.040	0.32	14.7(0.45)
	DEV (3)	8184	1.35	100.3	0.014	0.11	9.2(0.87)
Otindag	FOR (91)	10720	1.38	100.0	0.261	2.09	224.0(1.01)
sandy land	DEC (70)	9014	1.36	102.0	0.137	1.10	98.8(0.57)
	DEG (31)	7720	1.34	103.0	0.100	0.80	61.8(0.69)
	DEV (4)	10182	1.36	100.6	0.340	0.27	27.7(1.33)
Qubqi desert	FOR (93)	2560	1.36	101.2	0.278	2.22	57.0(0.78)
	DEC (75)	3262	1.35	102.3	0.146	1.17	38.1(1.25)
	DEG (32)	3289	1.35	102.4	0.244	1.95	27.9(0.89)
	DEV (4)	1136	1.34	104.3	0.037	0.30	3.4(2.1)

Table 2. (cont'd).

Sandy lands[a] region	Type (vegetation cover %)[b]	Area (km^2)	Bulk density ($mg\ m^{-3}$)	Mean depth ($m\ 10^{-2}$)	Organic matter (%)	Mean org-C ($kg\ m^{-2}$)	Total carbon (Tg C)(SD)
Tengger sand desert	FOR (97)	17865	1.30	106.0	0.377	3.00	539.1(1.56
	DEC (76)	1368	1.32	104.4	0.244	1.95	26.7(1.78)
	DEG (35)	6942	1.33	103.7	0.145	1.16	80.6(1.06)
	DEV (8)	288	1.32	105.0	0.046	0.37	1.1(1.08)
Badain Juran sand desert	FOR (98)	2036	1.28	108.0	0.519	4.15	84.6(0.56)
	DEC (73)	560	1.31	105.1	0.273	2.18	12.2(0.23)
	DEG (37)	2272	1.30	106.0	0.198	1.58	36.0(0.58)
	DEV (6)	1824	1.29	106.1	0.068	0.54	9.9(0.76)
Desert in Qaidam Basin	FOR (99)	3520	1.35	102.0	0.690	5.50	194.4(1.08)
	DEC (77)	1130	1.38	99.9	0.195	1.56	17.7(1.26)
	DEG (32)	1824	1.34	103.0	0.086	0.69	12.6(0.57)
	DEV (6)	1440	1.33	103.7	0.055	0.44	6.3(0.69)
Gurbang Tunggut desert	FOR (97)	2806	1.36	101.4	0.285	2.28	64.0(1.07)
	DEC (78)	952	1.32	104.5	0.150	1.20	11.4(1.25)
	DEG (31)	5296	1.32	104.3	0.109	0.87	46.2(1.33)
	DEV (2)	–	–	–	–	–	–
Taklimakan sand desert	FOR (98)	12690	1.33	103.7	0.305	2.44	309.8(0.57)
	DEC (72)	2408	1.37	100.8	0.161	1.29	31.0(0.78)
	DEG (32)	14200	1.38	99.3	0.117	0.93	133.0(0.45)
	DEV (1)	7615	1.37	100.7	0.040	0.32	24.4(0.89)
MEAN	FOR	158000	1.35	–	–	–	4895
	DEC	80960	1.35	–	–	–	2206
	DEG	60677	1.38	–	–	–	630
	DEV	34805	1.34	–	–	–	110
TOTAL		334442					7841

[a]Location of sites shown in Fig. 1.

[b]FOR, forerunner, latent desertification-prone land; DEC, decayed, lands under on-going desertification; DEG, degenerated, severe desertification-prone lands; DEV, devastated, most severe desertification-prone lands.

The percentage of desertification which can attributed to human economic activities, P_i, was calculated as

$$P_i = \{A_e[1 - E_t - E_p + (E_t E_p)]) + A_c[1 - C_p - C_t - (C_p C_t)] + A_w[1 - W_p - W_t - (W_p W_t)]\}/A_r, \quad (5)$$

where

A_e, A_c and A_w are the areas of desertification-prone lands in northeast, north central and northwest China, respectively;

E_t, C_t and W_t are the rates of increase/decrease in desertification-prone lands linked to temperature variations in northeast, north central and northwest China, respectively;

E_p, C_p and W_p are the rates of increase/decrease in desertification-prone lands linked to precipitation variations in northeast, north and northwest China; respectively, and

A_r is the total desertified area in this study region.

Soil bulk density was determined according to a known sample volume and oven-dry weight of the sample material (Hillel, 1982). Forty-year mean precipitation, AT and soil bulk density data were used in an attempt to develop significant ($p < 0.01$) MAXR multiple regressions linking these individual parameters and SOC.

Mean annual AT, winter (Jan.–Mar.), summer (Jul.–Sep.), nighttime (20:00–8:00) and daytime (8:00–20:00) air temperatures along with precipitation for the regions of northeast, north central and northwest China were obtained for the years 1950 through 1990 (Wang et al., 1998b; Zhai et al., 1999). We also

analyzed the climatological trends and variations of the three regions (Fig. 1). Long-term historical data for the three regions came mainly from 66 existing meteorological observation stations (Wang et al., 1998a), with 65 data records being complete from 1960 to 1990 and 53 being complete from 1951 to 1960. Outliers beyond three standard deviations were removed. In cases where a station was relocated, the earlier portion of the time series was shifted according to the difference in mean values before and after the relocation. The meteorological data from the three meteorological observation stations nearest to an individual SOC sampling site were used to relate meteorological parameters with SOC. Monthly and seasonal climatological means were computed separately for daytime (based on 14:00 local time data), and for nighttime (based on 2:00 local time). Farmland and population data were obtained from the China Statistics Bureau.

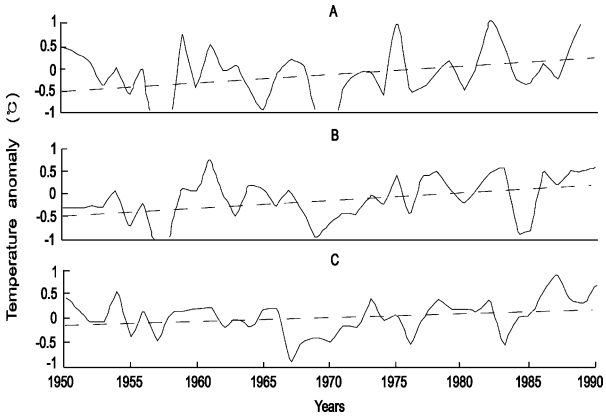

Fig 2. Annual anomaly time series of temperature: dashed lines indicate trends; A: northeast China; B: north central China; and C: northwest China.

3. Results

3.1. SOC variations

For the entire range of soils and areas tested, storage of soil carbon as organic matter on a whole profile basis averaged 2.34 kg C m^{-2} in the 0–1.0 m (Table 2), which is within the range of 2.2–7.3 kg C m^{-2} calculated for desert scrub and desert grassland by Schlesinger (1982). However, it is much lower than the value of 4.00 kg C m^{-2} calculated by Wu et al. (2003), for China, mainly due to the extended arid and semiarid regions in our study. Indeed, 4.895, 2.206, 0.630 and 0.110 Pg of organic carbon were housed, in the top 1.0-m soil layer of forerunner, decayed, degenerated and devastated lands (Table 2), respectively. The organic carbon content and organic carbon storage in the 0–1.0-m profile of the semihumid regions of desertified lands declined by region in the order northeast, north central, northwest, whereas for the 0–0.2-m profile the order was northeast, northwest, north central (Feng et al., 2002).

The details of annual increases in area of individual types of desertification-prone lands have previously been calculated (Wen et al., 1993; Zhu and Cheng, 1994). Based on the present organic carbon content in desertified lands, total emissions of carbon into the atmosphere in the last 40 yr have been 2.168 Pg, representing 35.8% of the organic carbon in the 0–1.0-m soil layer. Over the past 40 yr, decayed, degenerated and devastated lands have released 0.787, 0.300 and 0.270 Pg C, respectively, the remainder coming from forerunner lands (Feng et al., 2002). According to our investigation, the northeast, north central and northwest areas have released 0.975, 0.886 and 0.307 Pg C, respectively, in the last four decades (Feng et al., 2002).

3.2. Temperature and precipitation changes

Figure 2 shows the annual mean surface air temperature anomalies (SATA) in northwest, north central and northeast China, respectively. One cold period, from the 1960s through the 1970s, is common to all three regions (Fig. 2). The mean AT in northeast China remained relatively stable from the 1950s to the mid 1970s but rose thereafter by $\sim$1.0° (Fig. 2A). In north central China, temperatures remained low from the 1950s to the 1960s, with a warming trend beginning in the 1980s. The largest change in mean AT, roughly +1.5°, occurred between the mid 1950s and late 1990s, which supports the conclusion that most of northern China (except northwest China) has experienced severe and prolonged dry periods since the late 1990s (Zou et al., 2005; Fig. 2B). In northwest China the coldest period occurred from the 1960s to the mid 1970s, with temperatures gradually increasing since the 1980s (Fig. 2C). While aridity in the northeast has continued to worsen since the 1970s, in the north central region, dry conditions were mainly limited to the 1980s, and severe drought conditions in the northeast were limited to a period from the late 1970s to the early 1990s (Qian and Zhu, 2001).

Between 1950 and 1990 mean AT has increased on average by 0.14°, 0.28° and 0.15° $decade^{-1}$ in the northwest, northeast and north central regions (Fig. 3). During this period, summer temperatures showed no statistically significant regional trends, besides an increase of 0.09° $decade^{-1}$ in the northeast. However, during winter the northeast and northwest showed significant

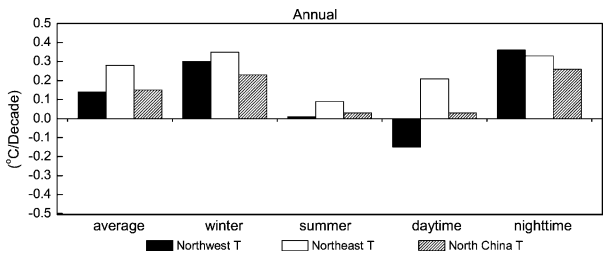

Fig 3. Decadal regional trends in daytime and nighttime, summer and winter season and mean temperature (°C) for 1950-1990 in desertified lands in China. Trends significant at the 5% confidence level.

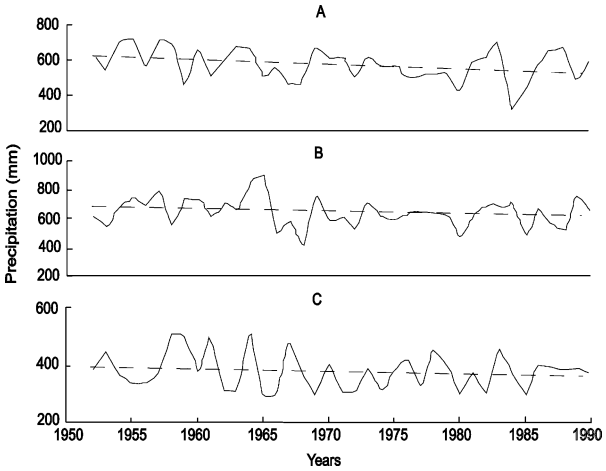

Fig 4. Time series of precipitation (mm) from 1950 to 1990 in different regions of the desertified lands in China. The dashed lines show the trends in precipitation. A: Northeast China (NE); B: north central China (NC); C: northwest China (NW).

($p \leq 0.05$) temperature increases of 0.35° and 0.30° decade^{-1}, respectively. For the same period nighttime temperatures increased by 0.36°, 0.33° and 0.26° decade^{-1} and daytime temperatures varied by −0.15°, +0.20° and +0.02° decade^{-1} in the northwest, northeast and north central regions, respectively (Fig. 3). Overall the mean winter and nighttime temperatures have risen in all three regions since 1950, whereas no such warming occurred in the summer in any of the three regions and, finally, daytime temperatures were slightly but significantly colder in the northwest region (Fig. 3; Wang and Gaffen, 2001). Trends of decreasing diurnal temperature were found in mainland China as a whole during the period of 1961–2000, with stronger decreases in northeast China, central South China region (Qian and Lin, 2004).

In the northeastern region of China precipitation was above normal from 1950 to the early 1960s, while in the late 1960s it dropped below the normal (Fig. 4). Over the entire study period from 1950 to 1990, precipitation in the region decreased by 25 mm decade^{-1} (Fig. 4A). The changes in precipitation in the north central region were similar to those in the northeast, with an overall decrease of 21 mm decade^{-1} (Fig. 4B). In the northwest mean annual precipitation was less than 400 mm, with a drop in precipitation of 10 mm decade^{-1} from 1950 to 1990 (Fig. 4C). Nonetheless, periods of relatively high precipitation occurred in the northwest in the 1950s and 1960s, as well as during a short period in the 1980s (Qian and Zhu, 2001).

3.3. Correlations of SOC to physical parameters

The SOC content of both 0–0.2-m and 0–1.0-m profiles was positively correlated with mean annual precipitation. Similar relationships have been reported for Arizona soils (Schlesinger, 1982). Precipitation explained more variation in SOC in the 0–1.0-m profile ($0.36 < \gamma^2 < 0.58$) than any other single variable (Table 3), while, by contrast, evaporation explained more variation in SOC for the 0–0.2-m profile ($0.20 < \gamma^2 < 0.44$; Table 3). As elevation is strongly linked to vegetative cover and depth of the ground water table, it is not surprising that SOC in

Table 3. Some linear regressions between SOC contents of profile and precipitation, mean air temperature, land elevation, or evaporation

Independent variables		0–0.1 m soil profile		0–0.2 m soil profile	
Land type	Parameter correlated	Correlation coefficient (r^2)	Slope	Correlation coefficient (r^2)	Slope
Forerunner	Precipitation (mm)	0.36	30.38	0.13	46.50
	Mean temperature (°C)	0.00	−0.02	0.03	−0.38
	Evaporation (mm)	0.14	−0.003	0.30	−0.002
	Land elevation (m)	0.07	−0.05	0.18	−0.24
Decayed	Precipitation (mm)	0.58	67.60	0.18	67.98
	Mean temperature (°C)	0.00	−0.04	0.15	−1.23
	Evaporation (mm)	0.27	−0.002	0.44	−0.002
	Land elevation (m)	0.03	−0.36	0.12	−0.24
Degenerated	Precipitation (mm)	0.44	79.80	0.14	143.16
	Mean temperature (°C)	0.02	−0.31	0.08	−2.13
	Evaporation (mm)	0.31	−0.002	0.20	−0.0004
	Land elevation (m)	0.28	−2.08	0.03	−0.30
Devastated	Precipitation (mm)	0.53	252.75	0.15	218.26
	Mean temperature (°C)	0.00	−0.41	0.50	−11.88
	Evaporation (mm)	0.32	−0.001	0.40	−0.0003
	Land elevation (m)	0.06	−17.32	0.15	−1.44

[a]See Table 1 for land type designations forerunner-devastated.

Table 4. Linear regressions relating SOC (1360 numbers) in the top 1-m soil profile to precipitation (P) (4080 numbers), or diurnal and seasonal temperatures (°C) (4080 numbers) in different desertified lands of China

Land type region[a]		Mean air temperature (°C)					Precipitation (mm) (slope)
		Daytime (slope)	Nighttime (slope)	Winter (slope)	Summer (slope)	Mean (slope)	
Forerunner[b]	NE	0.06	0.34 (−0.3129)	0.30 (−0.1872)	0.06	0.01	0.00
	NC	0.72 (0.7038)	0.08	0.00	0.06	0.48 (−1.1217)	0.82
	NW	0.50 (−0.1383)	0.00	0.01	0.60 (−0.2411)	0.57 (−0.3171)	0.29 (0.0139)
	All	0.05	0.32 (−0.5858)	0.09	0.05	0.01	0.46
Decayed	NE	0.08	0.29 (−0.1627)	0.26	0.14	0.01	0.00
	NC	0.73 (0.4646)	0.08	0.00	0.06	0.50 (−0.7418)	0.82
	NW	0.03	0.46 (−0.1316)	0.11	0.00	0.00	0.14
	All	0.11	0.24 (−0.3001)	0.08	0.02	0.00	0.58
Degenerated	NE	0.19 (0.1158)	0.05	0.04	0.02	0.02	0.00
	NC	0.60 (0.2296)	0.03	0.05	0.00	0.46 (−0.3916)	0.71
	NW	0.01	0.54 (−0.1152)	0.13	0.37	0.05	0.11
	All	0.06	0.24 (−0.3001)	0.06	0.00	0.00	0.44
Devastated	NE	0.14	0.04	0.09	0.00	0.01	0.51
	NC	0.7 (0.1024)	0.07	0.02	0.06	0.49 (−0.1658)	0.84
	NW	0.08	0.26	0.03	0.03	0.15	0.03
	All	0.08	0.25	0.09	0.01	0.00	0.53

[a]NE = northeast; NC = north central = north China; NW = northwest; All = NE, NC and NW combined.
[b]See Table 1 for land type designations forerunner, decayed, degenerated and devastated.

the 0–0.2-m and 0–1.0-m soil profiles was inversely correlated to elevation (Table 3). The mean AT explained additional variation in the SOC in the 0–0.2-m profile, but no other individual parameter showed a significant correlation with SOC for the 0–1.0-m profile.

In forerunner lands and decayed lands of the northeast, SOC was negatively correlated with nighttime AT and winter AT, while in degenerated lands SOC was positively but weakly correlated with daytime AT ($\gamma^2 = 0.19$; Table 4). In the north central region, SOC was positively correlated with daytime AT ($0.60 < \gamma^2 < 0.73$) as well as mean AT with land types ($\gamma^2 =$ 0.46–0.50). However, in the northwestern regions, relationships between SOC and temperature were more closely related to the degree of land desertification (Table 4). Seasonal and day/night temperatures fluctuations can apparently lead to a significant variation in SOC, which can, in turn, potentially affect regional climate change and ultimately natural ecosystems.

In the northeastern region, for every 1° increase in winter temperatures, the SOC of forerunner and decayed lands increased by nearly 10% on a relative basis, while for nighttime temperatures the increase was 5% on a relative basis (Table 4). A mean of 45% of total SOC-derived emissions came from the northeastern region, which also accounted for nearly 30% of the total lands deteriorated in the past 40 yr. In the north central region, for every 1° increase in mean daytime temperature, the SOC of forerunner, decayed, degenerated and devastated lands increased by 16, 14, 17 and 14%, respectively, while increases for mean AT were 26, 24, 30 and 25%. Land desertification in north China accounted for 28% of deteriorated lands. In the past 40 yr, their SOC-derived greenhouse gas emissions have accounted for 46% of total emissions. The SOC of decayed, degenerated and devastated lands in the northwest showed a significant positive correlation with nighttime AT ($0.27 < \gamma^2 < 0.54$), however, the SOC of forerunner lands was negatively correlated with

the daytime and summer AT. For each 1° increase in nighttime AT○, the SOC of decayed, degenerated and devastated lands in the northwest rose by 8, 12 and 6% (relative basis), while for each 1° increase in daytime and summer temperature, the SOC of northwestern decayed lands decreased by 2% (relative basis). As emissions from SOC in the northwest region represent 9% of total emissions, even if the region accounts for 42% of Chinese lands under desertification on an areal basis, it is much less important a region in terms of greenhouse gas emissions than its counterparts.

Based on these estimates and AT trends in the different regions, one can estimate that over the past four decades, the northeast, north central and northwest regions have released 0.975, 0.886 and 0.307 Pg C, respectively. In the northeast about 20% of emissions from SOC were attributable to AT increases, particularly those of nighttime and winter AT; in the north central region about 31% of emissions from SOC were attributable to precipitation and 16% to mean AT increases; while in the northwest about 28% of emissions from SOC were attributable to increasing mean AT, 18% to increasing nighttime AT, and 32% to decreasing precipitation (Fig. 4).

3.4. Correlations of SOC to desertification-prone lands

Over the past four decades, some 176 000 km^2 of arid lands in northern China have deteriorated into desertified lands under the influence of anthropogenic factors. Based on eq. (5) we estimate human activities in northern China to have accounted for 47% of emissions from SOC.

The total quantity of carbon sequestered in the top 1.0-m profile during the last 40 yr has been 0.644 Pg, representing 8.2% (relative basis) of the organic carbon currently remaining in the 0–1.0-m soil layer (Feng et al., 2001b). The net carbon released into the atmosphere in the past 40 yr would thus amount to 2.168 Pg, or the equivalent of 7.949 Pg of CO_2. The remaining land area, that has neither been desertified nor rehabilitated, but is prone to desertification accounts for about 158 000 km^2. It contains 4.895 Pg C, equivalent to 177% of the carbon released between 1950 and 1990. These land areas should be managed carefully to minimize future organic matter losses.

Based on 1990 estimates of organic carbon contents in soils of desertified lands, and current trends, total emissions of carbon into the atmosphere up to 2030 could total 1.996 Pg C, of which decayed, degenerated and devastated lands would contribute 0.988, 0.490 and 0.518 Pg, respectively. These total carbon emissions would represent 25.45% of the organic carbon currently in the 0–1.0-m profile. By 2030 some 55 030 km^2 of different types of desertification-prone lands will have been rehabilitated. Thus 0.753 Pg C may be sequestered in the top 1.0-m soil by 2030, representing 9.6% of the total carbon currently in the 0–1.0-m soil profile.

4. Discussion

4.1. Physical parameter impact

While there was considerable variation in carbon concentrations used to calculate SOC, differences in bulk density were small across the four desertified land types, thus having little effect on SOC (Feng et al., 2001b). Forerunner soils had higher carbon concentrations, organic matter contents and ultimately SOC than decayed soils. The devastated soils had lower organic matter contents and therefore lower carbon concentrations than degenerated soils (Schlesinger, 1982).

The variation in organic carbon storage in the top 1.0-m or 0.2-m soil layer were closely related to the vegetative cover index, which in turn is controlled by local climatic conditions. Consequently, sandy soils in humid and semihumid regions, which store larger amounts of organic carbon, would potentially release greater quantities of carbon into the atmosphere during the desertification process than would semiarid or arid lands.

Uncertainty in SOC content arises from uncertainties in measurements made during the different mapping and soil surveying programmes undertaken over the decades. Such an uncertainty (error) was assigned to each observation based on a random selection from a normal distribution according to the standard deviation reported in the documentation consulted (Feng et al., 2002). In so doing individual predicted SOC values could be off by as much as 30%. The linear regression coefficients presented in Table 3 show that some parameters which correlate with SOC according to climate and altitude are reasonably satisfactory. However, the uneven geographical distribution of sampling sites, the slowly response of SOC to climate change and the fact that some biomass was underrepresented can all bias these relationships. Even more serious errors are introduced when the analysis is applied to spatial parameters in different climatic zones, where aspects of regional climate change are uncertain.

4.2. Climatic impacts

Elevated nighttime temperatures may have direct, but counterbalancing effects on SOC content through such mechanisms as carbon loss through increased rates of respiration during the warmer nights, and differential effects on photosynthesizing plants present under degenerated vs. devastated lands (Richard et al., 1999). Due to the low annual mean temperature (6.3°C) and short summer (50–60 days), the growth of vegetation in arid desertified lands of the northeast depends most strongly on temperature variations (Feng et al., 2001c). Elevated winter and nighttime temperatures can extend the frost-free period during which cold-resistant plants can grow, which can, in turn, reduce available soil moisture prior to the period of rapid growth of warm-season plants. The increasing density of invasive exotic forbs has been recognized as a threat to the function of numerous natural ecosystems (Wedin and Tilman, 1996; Cohen and

Carlton, 1998) and it has been linked to rises in nighttime and winter AT. Under these conditions, plant species normally available for livestock production decrease with a concomitant increase in temporal and spatial availability of nutrients, water and SOC, leading to an increase in the emission of greenhouse gasses from SOC.

However, in the north central region, where annual mean AT in most areas is higher (2.4°–10.8°) and annual mean precipitation (129–500 mm) much lower than in the northeast region, the growth of arid-adapted vegetation in desertified-prone lands depends first and foremost on precipitation and secondarily on the AT. Indeed, SOC is strongly and directly correlated with precipitation and inversely correlated with mean AT in these areas. Due to long-term low soil moisture content, the arid-adapted plants growing there depend strongly on the periodic precipitation (Zhu et al., 1998).

Correlations between temperature or precipitation and SOC were more highly significant when temperature or precipitation data were subdivided on a diurnal (nighttime vs. daytime), seasonal (summer vs. winter) or degree of land degradation (forerunner, decayed, degenerated and devastated) basis (Table 4).

Climatic conditions in the northwest are hyperarid, with the growth of arid-adapted plants being mainly dependent upon river and ground water. Consequently, the relationship between SOC and AT is a complex one. The SOC of forerunner lands was significantly correlated with daytime, summer and mean AT, whereas for other more degraded desertified lands significant correlations occurred with nighttime AT. The slight effect of precipitation on SOC occurred through its periodic influence on topsoil moisture, which determined the biomass of plants contributing to the SOC. High night AT increased the pre-daylight evaporation of soil water, contributing to greater soil aridity, a reduced coverage of arid-adapted plants and decreased accumulation of SOC, under the progressively decreasing precipitation and increasing temperatures of the region.

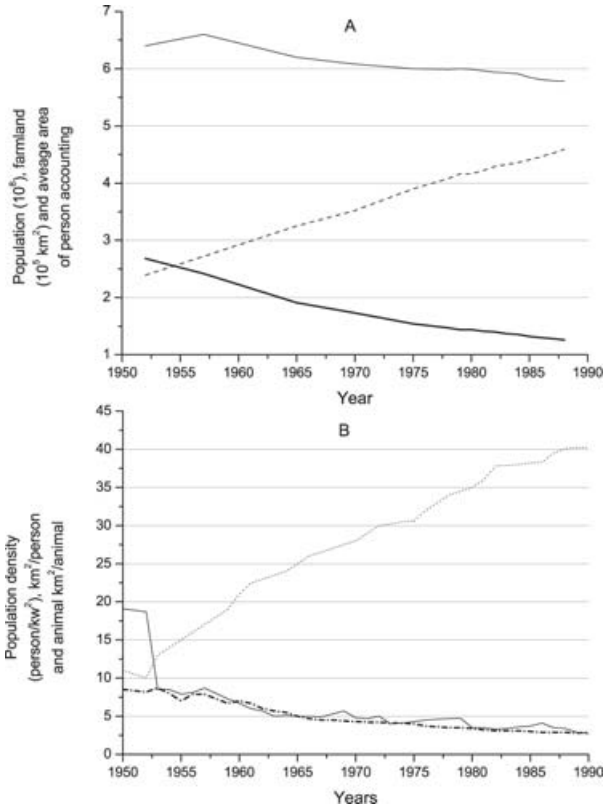

Fig 5. The area of farmland, population and mean area per person and per animal in northern China and Jirem Prefecture, inner Mongolia. A: North China; the area of farmland (light solid line), population (black dashed curve) and mean area *per capita* (black solid line) in north China; B: Jirem Prefecture, inner Mongolia; human population density (light dashed line), mean area *per capita* (black dashed curve) and per animal (black solid line) in Jirem Prefecture, inner Mongolia.

4.3. Anthropogenic impacts

Besides the influence of natural climatic variations on greenhouse gas emissions from SOC, excessive human activity, including overcultivation, overgrazing and undue harvesting of fuel wood, has, in past centuries, shown itself to be an important factor in the degradation of productive lands into desertified lands. Deteriorated ecosystems present fewer grass species, vegetative cover, soil nutrients and organic carbon content, leading to an increased release of SOC-bound carbon into the atmosphere.

In the last 4 yr, the growth in the portion of the northern Chinese human population (not considering the urban populations), which is supported by industry rather than agriculture, has risen at a rate of 1.8% yr^{-1} (Zhu et al., 1998; Fig. 5A). For instance, in the marginal dry-farming and steppe regions undergoing desertification, the mean rate of human population growth is as high as 3.28% yr^{-1}. The mean population density, which was 11.2 individuals km^{-2} in 1950, had risen to 40.5 individuals km^{-2} by 1990, even reaching 60 individuals km^{-2} in some regions (Zhu et al., 1998; Fig. 5B). In 1950, the mean land base for grazing livestock was 1.7–1.9 ha head^{-1}, but by 1990, this had declined to 0.30–0.37 ha head^{-1} (Fig. 5B). Figures 5A and 5B support the hypothesis that increased human and animal populations have imposed a significant pressure upon these lands and that as a result these arid lands have been severely deteriorated. Over the past four decades, some 176 000 km^2 of arid lands in northern China have deteriorated into desertified lands under the influence of anthropogenic factors. These include 44 700 km^2 of desertification-prone lands generated by overcultivation of steppe lands, 49 900 km^2 from overgrazing of steppe lands, 56 000 km^2 due to excessive collection of fuel wood, and 14 700 km^2 by misuse of water resources and irrational industrial and urban development (Zhu et al., 1998; Feng et al., 2002). The excessive economic activities are interrelated to the growth in the human population.

According to Zhu et al. (1998), about 90% of desertification-prone lands have been generated as a result of human economic activities.

Currently, land desertification in northern China is an ongoing process, but the rate is being controlled to some extent. About 10% of desertification-prone land has been rehabilitated to near their original soil carbon content, and 12% of all desertification-prone land has been improved to some extent (Zhu and Cheng, 1994). If traditional land-use techniques and systems are employed without scientifically based artificial remedial measures, the area of desertified land may yet increase by up to 249 700 km^2 by 2030 (Feng et al., 2002).

5. Conclusions

Organic carbon has a short residence time in soils and can be rapidly converted to greenhouse gases such as CO_2 under changing land-use patterns. In this study, we determined the variations in soil organic carbon over the period of 1950–1990 and predicted those likely to occur by 2030. The pool of organic carbon in desert soils accounts for approximately 7.7 and 4.0% (7.8 and 4.12 Pg C), respectively, of the total organic carbon sequestered in the 0–1.0-m and 0–0.2-m profiles of China's soils. Based on the SOC of China's desertified soils, the top 1.0 m of the world's desert soils, spread over an area of 1.8×10^9 km^2, house a pool of organic carbon estimated at 42.1–100.8 Pg C. This represents 3–7% of the total organic carbon in the world's soils (Schlesinger, 1977). Based on the present organic carbon content in desertified lands, total net emissions of carbon into the atmosphere during the last 40 yr (1950–1990) have been 2.168 Pg, representing 25.4% of the organic carbon in the 0–1.0-m soil layer.

Variations in the quantity of greenhouse gas emissions from SOC were closely linked to global warming, particularly to the rise in winter and nighttime AT in desertified land. Over the period of 1950–1990, according to correlation analysis, about 20% of emissions from SOC in the northeast were attributable to rises in AT, particularly nighttime and winter AT, while for north central and northwestern regions mean AT accounted for 28 and 18% of emissions, respectively. Due to the influences of global warming, precipitation was the most significant parameter in accounting for emissions from SOC in the north central and northwest regions. Decreasing precipitation over the four decades studied accounted for 31 and 32% of emissions from SOC in the north central and northwest regions, respectively.

Human activities, which overburdened the fragile environment of arid lands, were also noted as important factors accounting for emissions from SOC to the atmosphere. Urban and industrial development linked with the rapid rate of population growth (6.1% *per annum*) in northern China over the period of 1950–1990, has accelerated the deterioration of arid lands. A number of anthropogenic factors, prevalent between 1950 and 1990, account for the 176 000 km^2 of arid lands in northern China, which were degraded into desertified lands. The deterioration of the ecosystems ultimately resulted in 47% of total SOC in desertified lands being released into the atmosphere. Under continued global warming, if traditional land-use techniques and systems are employed without scientifically based remedial measures being implemented, the area of desertified land may increase by up to 249 700 km^2 by 2030, total net emissions reaching 1.243 Pg C. This suggests a serious potential for a global greenhouse effect.

Without a clear causal link, there is insufficient evidence to eliminate factors other than nighttime and winter AT as causes for the changes observed in greenhouse gas emissions from SOC. Unfortunately, few experiments or models designed to investigate climate-change effects have focused on manipulating winter and/or nighttime AT to achieving an increase in mean AT. Although the outcome of this study can support an intimation of future ecosystems dynamics should climate change continue to be manifested primarily as an increase of nighttime and winter AT, further investigation to define the relationships and underlying mechanisms existing between diurnal and seasonal temperatures and greenhouse gas emissions from SOC are imperative.

6. Acknowledgments

This research was supported by a grant from the Hundred Talent Scholar Foundation (2003401) and Key Project (KZCX3-SW-329) of Chinese Academy of Sciences.

References

Bon, H. L. 1976. Estimate of organic carbon in world soils. *Soil Sci. Soc. Am. J.* **40**, 468–472.

Bruce, J. P., Frome, M. and Haites, E. 1999. Carbon sequestration in soils. *J. Soil Water Conserv.* **54**, 382–389.

Burke, I. C., Yonker, C. M., Parton, W. J., Cole, C. V., Flach, K. and co-authors. 1989. Texture, climate, and cultivation effects on soil organic matter content in US grassland soils. *Soil Sci. Soc. Am. J.* **53**, 800–803.

Cohen, A. N. and Carlton, J. T. 1998. Accelerating invasion rate in a highly invaded estuary. *Science* **279**(5350), 555–558.

Emanuel, W. R., Shugart, H. H. and Stevenson, M. P. 1985. Climatic changes and the broad-scale distribution of terrestrial ecosystem complexes. *Climatic Changes* **7**, 29–30.

Fang, J. Y., Chen, A. P., Peng, C. H., Zhao, S. Q. and Ci, L. J. 2001. Changes in forest biomass carbon storge in China between 1949 and 1998. *Science* **292**, 2320–2322.

Feng, Q., Cheng, G. D. and Endo, K. H. 2001a. Carbon storage in desertified lands: A case study from north China. *GeoJournal* **51**, 181–189.

Feng, Q., Cheng, G. D. and Mikami, M. S. 2001b. The carbon cycle of sandy lands in China and its global significance.*Climatic Change* **48,** 535–549.

Feng, Q., Cheng, G. D. and Endo, K. H. 2001c. Water content variation and respective ecosystem of sandy land in China. *Environ. Geol.* **40**(9), 1075–1083.

Feng, Q., Endo, K. H. and Cheng, G. D. 2002. Soil carbon in desertified land in relation to site characteristics. *Geoderma* **106**(1–2), 21–43.

Hillel, D. 1982. *Negev: Land, Water and Life in a Desert Environment*. Praeger, New York, 56–78.

Kern, J. S. 1994. Spatial patterns of soil organic carbon in the contiguous United States. *Soil Sci. Soc. Am. J.* **58**, 438–448.

Lal, R. 1999. World soils and the greenhouse effect. *IGBP Newsl.* **37**, 4–5.

Li, Z. P. and Wang, X. J. 1998. Simulation of soil organic carbon dynamics under changing landuse pattern in hilly red soil region. *Chin. J. Appl. Ecol.* **9**, 365–370 (in Chinese).

Li, Z. and Zhao, Q. G. 2001. Organic carbon content and distribution in soils under different land use in tropical and subtropical China. *Plant Soil* **231**, 175–185.

Peng, C. H. and Apps, M. J. 1997. Contribution of China to the global carbon cycle since the last glacial maximum. *Tellus* **49B**, 393–408.

Qian, W. H. and Lin, X. 2004. Regional trends in recent temperature indices in China. *Climate Res.* **27**, 119–134.

Qian, W. H. and Zhu, Y. F. 2001. Climatic change in China from 1880 to 1998 and its impact on the environmental condition. *Climatic Change* **50**, 419–444.

Richard, D. A., James, K. D. and Daniel, G. M. 1999. Grassland vegetation changes and nocturnal global warming. *Science* **283**, 229–231.

SAS Institute. 1985. *SAS/STAT Guide for Personal Computers* Version 6. SAS Inst., Cary, NC.

Schlesinger, W. H. 1977. Carbon balance in terrestrial detritus. *Annu. Rev. Ecol. Syst.* **8**, 51–72

Schlesinger, W. H. 1982. Carbon storage in the Caliche of arid soils: A case study from Arizona. *Soil Sci.* **133**, 247–255

Schlesinger, W. H. 1984. Soil organic matter: Sources of atmospheric CO_2. In: *Role of Terrestrial Vegetation in the Global Carbon Cycle, Measurement by Remote Sensing* (ed. G. M. Woodwell). John Wiley and Sons, New York, 11–127.

Schlesinger, W. H., Reynold, J. F., Cunningham, G. L., Huenneke, L. F., Jarrell, W. M. and co-authors. 1990. Biological feedbacks in global desertification. *Science* **247**, 1043–1048.

van Bemmelen, J. W. 1890. Die Zusammenetzung des Meeresschlicks in den neuen alluvien des Zuiderzee (Niederlands). *Landw. Vers. Sta.* **37**, 239–256 (in German).

Vogt, K. A., Vogt, D. J., Brown, S., Tilley, J. P., Edmonds, R. L. and co-authors. 1995. Dynamics of forest floor and soil organic matter accumulation in boreal, temperate, and tropical forests. In: *Soil Management and Greenhouse Effect* (eds.R. Lal et al.) CRC Press, Boca Raton, FL, 159–178.

Wang, J. L. and Gaffen, D. J. 2001. Late-twentieth-century climatology and trends of surface humidity and temperature in China. *J. Climate* **14**, 2833–2845.

Wang, W., Zhang, J. and Wang, W. 1998a. A study on organic matter balance in farmland in Huang-Huai-Hai Plan. *Sci. Agric. Sin.* **21**, 19–26 (in Chinese).

Wang, S. W., Ye, J. L., Gong, D. Y. and Zhu, J. H. 1998b. Construction of mean annual temperature series for the last one hundred years in China. *Q. J. Appl. Meteorol.* **9**, 392–401 (in Chinese).

Wedin, D. A. and Tilman, D. 1996. Influence of nitrogen loading and species composition on the carbon balance of grasslands. *Science* **274**, 1720–1723.

Wen, Y. P., Xu, X. B. and Shao, Z. Q. 1993. Measurement of atmospheric baseline CO_2 with a non-disperse infrared analyzer. *Q. J. Appl. Meteorol.* **24**, 476–480.

Wolff, E. 1864. Entwurf zur bodenanalyse. *Ztschr. Anal. Chem.* **3**, 83–115.

Wu, H. B., Guo, Z. T. and Peng, C. H. 2003. Land use induced changes of organic carbon storage in soils of China. *Global Change Biol.* **9**, 305–315.

Zhai, P. M., Sun, A. J., Ren, X. L., Gao, B. and Zhang, Q. 1999. Changes of climate extremes in China. *Climatic Change* **42**, 203–218.

Zhu, Z. D. and Cheng, G. T. 1994. *Sandy Land Desertification in China*. Sciences Press, Beijing, 87–102 (in Chinese).

Zhu, Z. D., Di, X. M. and Liu, S. 1988. *Desertification and Rehabilitation in China.* Sciences Press, Beijing, 222–223 (in Chinese).

Zhu, Z. D., Zhang, X. L. and Lin, Y. Q. 1998. *Sandy Land Rehabilitation, Engineering and Technology*. Chinese Environmental Sciences Press, Beijing, 139–149 (in Chinese).

Zou, X., Zhai, P. and Zhang, Q. 2005. Variations in droughts over China: 1951–2003. *Geophys. Res. Lett.* **32**, L04707, doi:10.1029/2004GL021853.